Wise Observatory's H_α filters

Spectral Verification

Oded Spector, September 2006

This document describes the tests that were performed in order to verify the spectral behavior of the Wise observatory's H_α filters, and summarizes these tests' results.

1 The Filters

The ten H_α filters of the wise observatory are listed in the following table:

Name	Additional Label	Shape
H_α 1	6447, continuum, MicroCoatings 645nm ∅QED	round ∅50.9mm
H_α 2	6562, v=0 km/s, MicroCoatings 656.3nm ∅QEC	"
H_α 3	6586, v=1050 km/s, MicroCoatings 659nm ∅PES	"
H_α 4	6610, v=2150 km/s, MicroCoatings 661.5nm ∅QEB	"
H_α 5	670nm normal, 669nm @f/4, v=6240 km/s, MicroCoatings 670nm ∅PEY, spectral curve prepared for this unit	"
H_α 6	NB, 6635, PO# 06-00360, ∅50.9mm, CWL @ 663.5nm, FWHM=5.5nm	"
H_α 7	NB, 6697A, PO# 06-00360, ∅50.9mm, CWL @ 668nm, FWHM=5.5nm	"
H_α 8	NB, 6760, PO# 06-00360, ∅50.9mm, CWL @ 676nm, FWHM=6.0nm	"
H_α 9	NB, 6800, PO# 06-00360, ∅50.9mm, CWL @ 680nm, FWHM=6.5nm	round ∅50.9mm
RGO 67	H_α , v=4390km/sec, 6659, Schott	square

Table 1 – Wise Observatory H_α filters

These filters are used for measuring H_α (Balmer alpha) line emission with a wide range of redshifts, and the continuum emission near this line. Since the H_α line is strongly emitted from starburst areas, this serves as an effective tool for measuring star formation rates (SFR).

2 Test Procedure

The spectral properties of the filters were measured using the Jasco V-530 UV/VIS spectrometer of the applied physics group (used with the courtesy and help of Prof. Abraham Katzir and Dr. Lev Nagli). The measurements were made on August 6, 2006.

Transmittance curves for all filters were measured in the range 6300Å to 7000Å, with a resolution of 2Å. For each filter, several measurements were made for several points in the filter's surface.

The raw data was then analyzed, and parameters such as $\lambda_{central}$ (CWL – Central Wavelength), FWHM (Full Width at Half Maximum) and T_{max} (peak transmittance) were calculated. By comparing results through different points in each filter, uniformity was tested.

Additionally, some points in the filters were measured more than once, and some measurements were taken without a filter. These were used for estimating the measurement error.

Blocking outside the transmitting band was estimated, by averaging over the transmittance at wavelengths far from it. Wavelengths which were more than 5×FWHM away from the central wavelength (CWL) were included in this calculation (except for filter "RGO 67" for which 4×FWHM was used). This wavelength distance is not far enough, as the transmittance still seems to decline with the distance from the CWL. However, it was not possible to increase this distance, since data was not gathered at farther wavelengths. Therefore, the blocking results can only serve as a transmittance upper limit estimate.

3 Results

3.1 Visual Inspection

All of the filters have two distinctively different sides: one red, and the other shining silver.

Visual inspection of the filters showed that some of them have dull (matt) spots on the silver side. These spots differ in size and location, but most of them are round and located at the center of the filter.

The following table describes the visual spot on each of the filters (or "-" for no detected spot):

Name	Spot Description
H_α 1	A round spot at the center of the silver side, which radius is about 2/3 of the filter's radius
H_α 2	A round spot at the center of the silver side, which radius is about 1/2 of the filter's radius
H_α 3	A round spot at the center of the silver side
H_α 4	A round spot at the center of the silver side
H_α 5	A round spot at the center of the silver side, which covers most of the filter's area
H_α 6	–
H_α 7	–
H_α 8	–
H_α 9	A very dull spot that covers the outer part of the filter - roughly all the area, which distance from the filter's center is more than about 1/2 of the filter's radius
RGO 67	–

Table 2 – Visual Spots on the filters

3.2 Transmittance Curves

The following figures show all the measured transmittance curves, each filter in a separate figure with all its measurements. However, for some of the filters ("H_α 1", "H_α 2" and "H_α 5") all measured

curves were too similar to be shown separately, and so only one curve is shown for each (the average of the measured curves).

Descriptions of the points in the filters, for which each of the measurements were taken, are listed in Table 3.

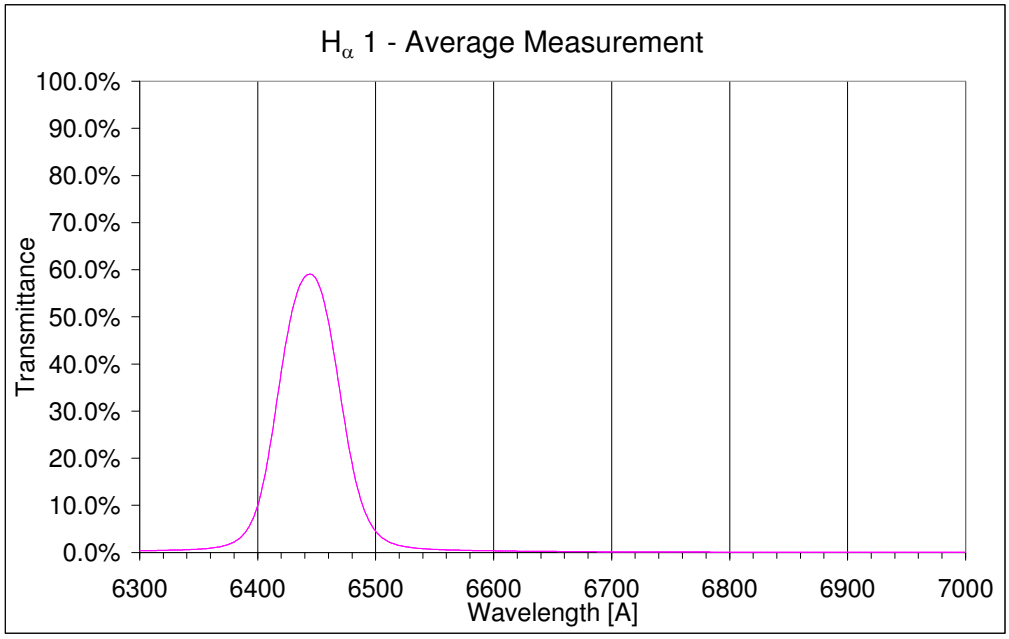

Figure 1 – Transmittance of filter H_α 1

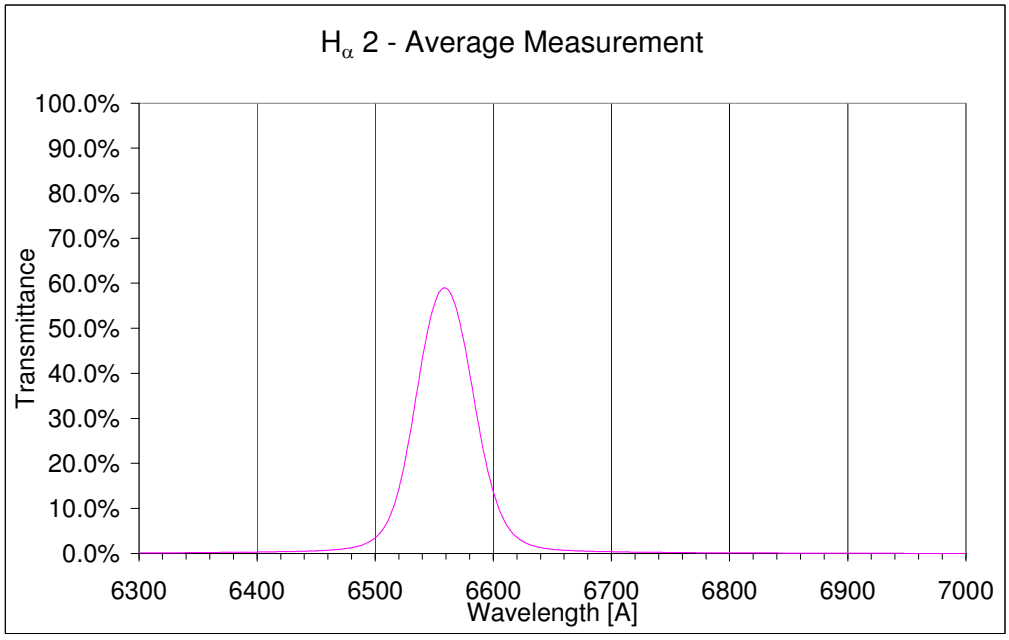

Figure 2 – Transmittance of filter H_α 2

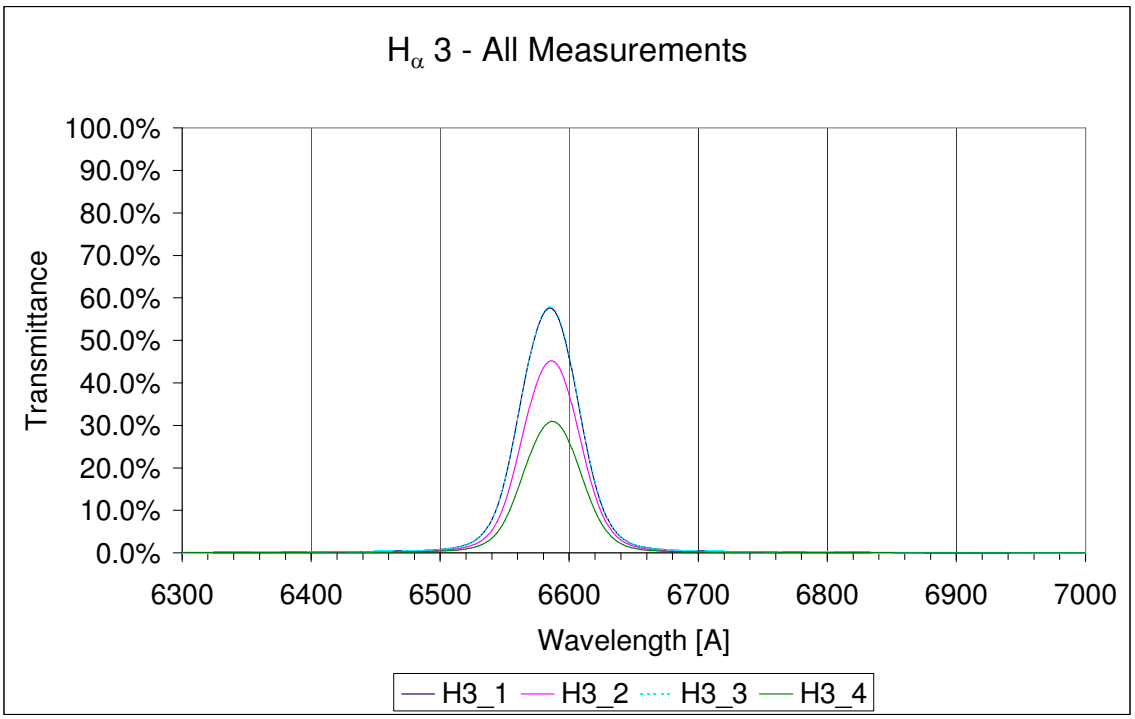

Figure 3 – Transmittance of filter H_α 3

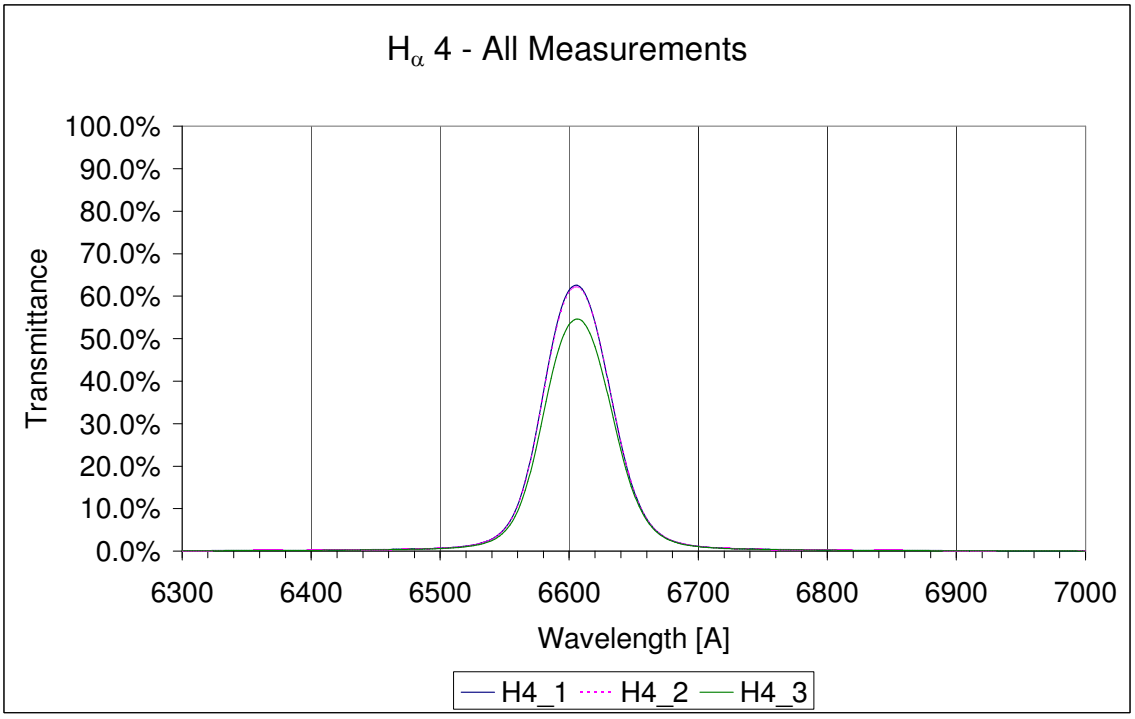

Figure 4 – Transmittance of filter H_α 4

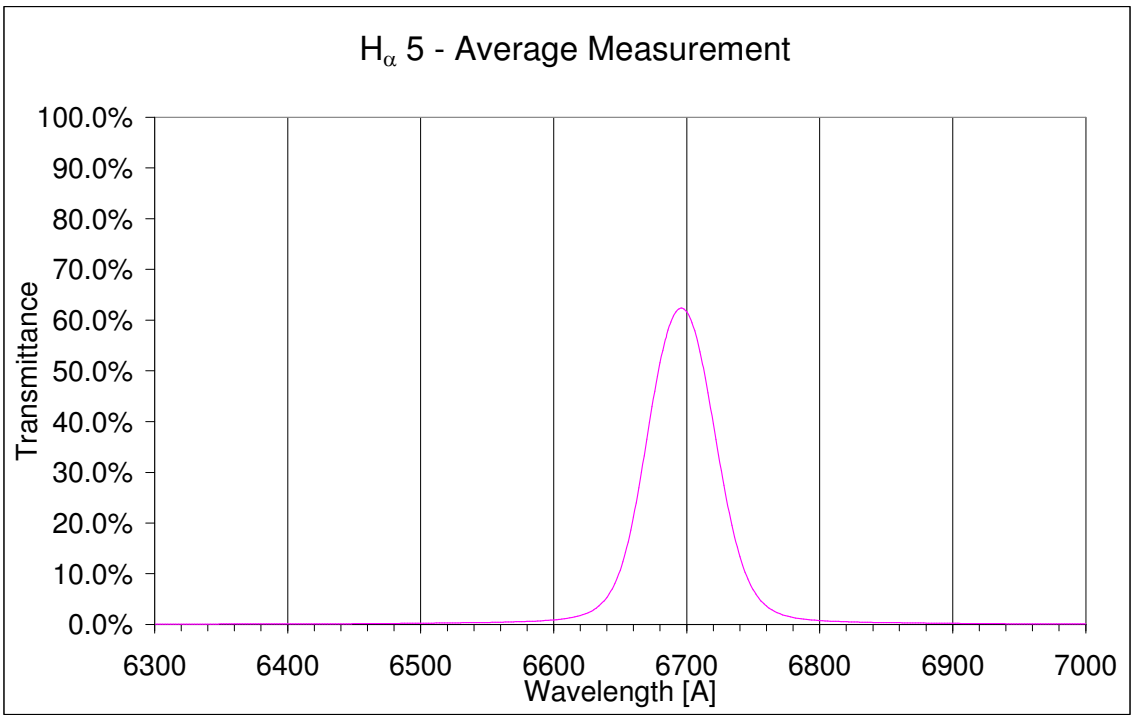

Figure 5 – Transmittance of filter H_α 5

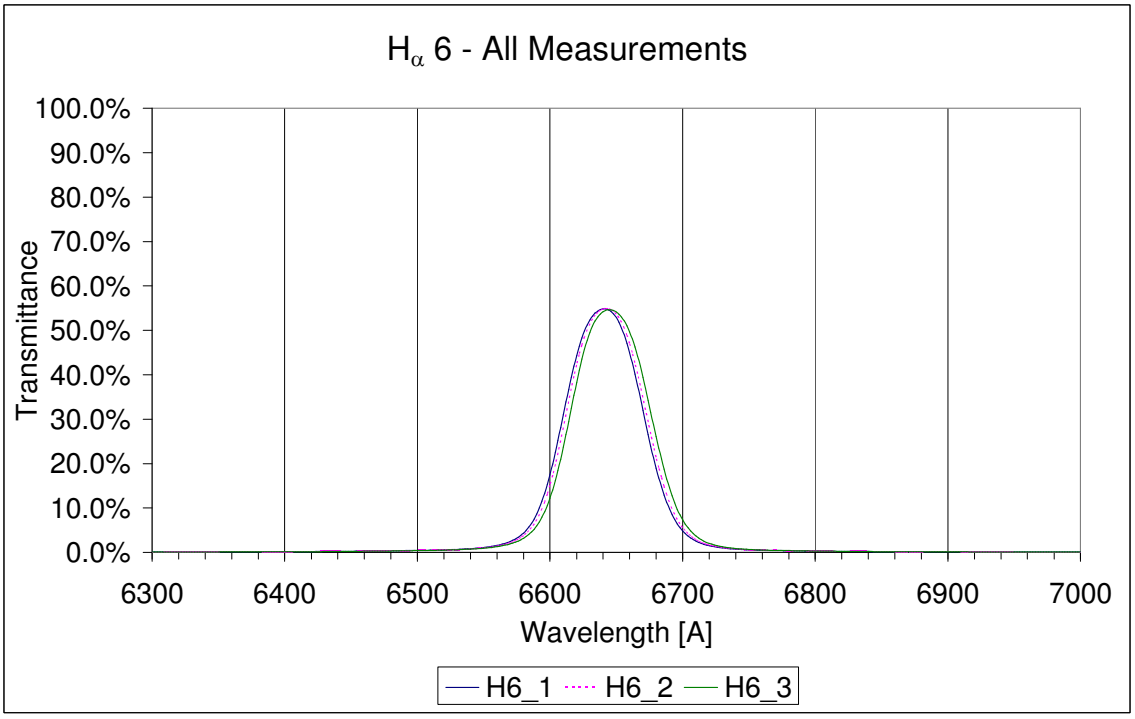

Figure 6 – Transmittance of filter H_α 6

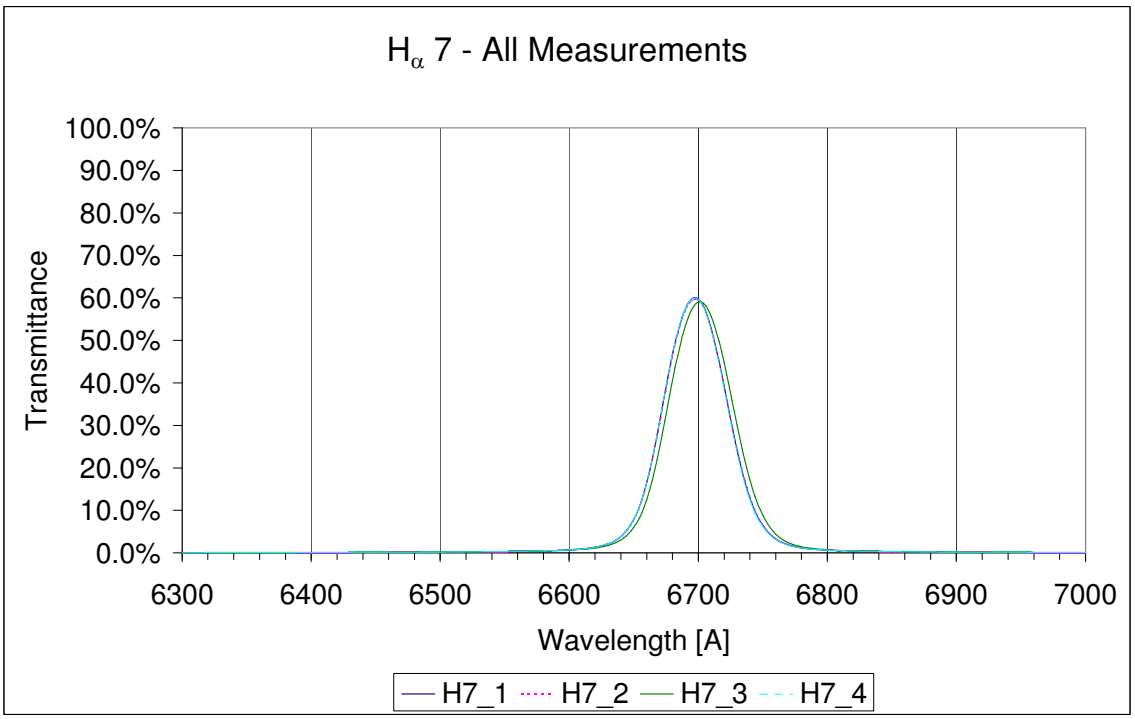

Figure 7 – Transmittance of filter H_α 7

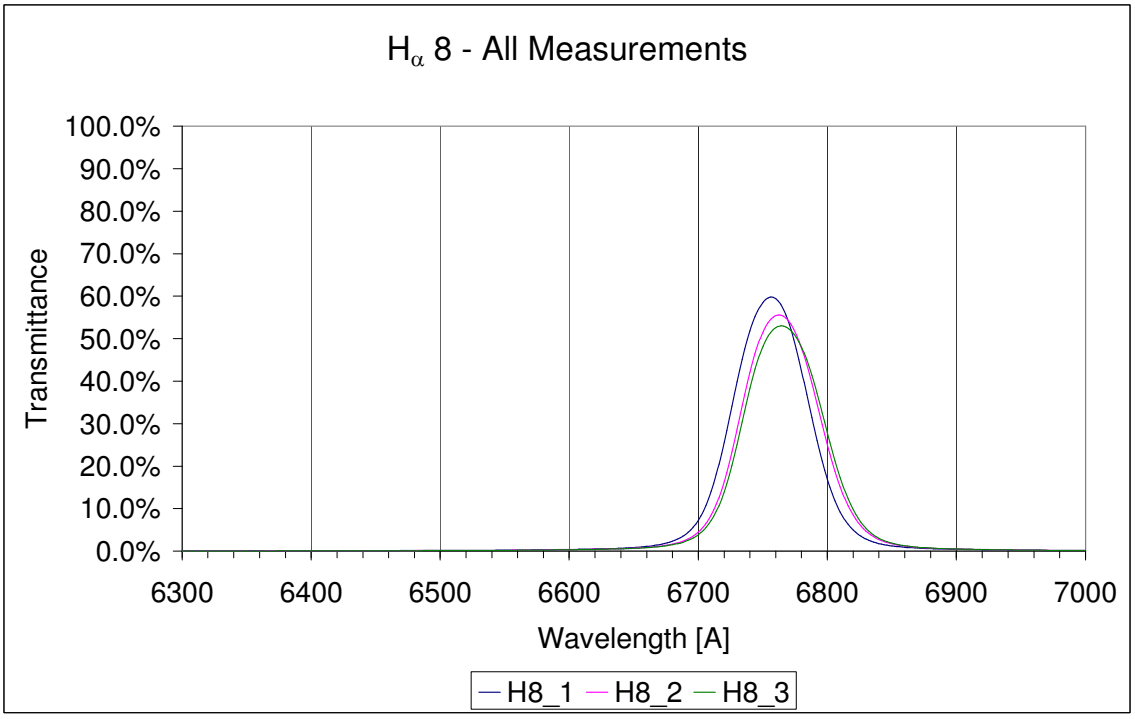

Figure 8 – Transmittance of filter H_α 8

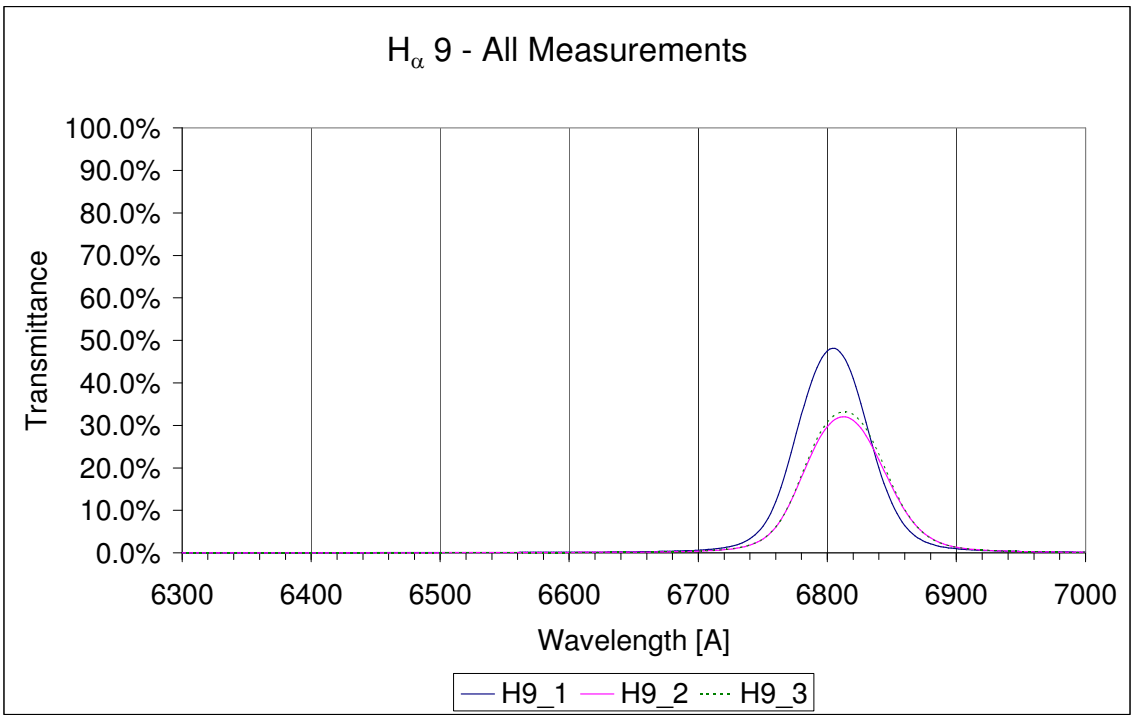

Figure 9 – Transmittance of filter H_α 9

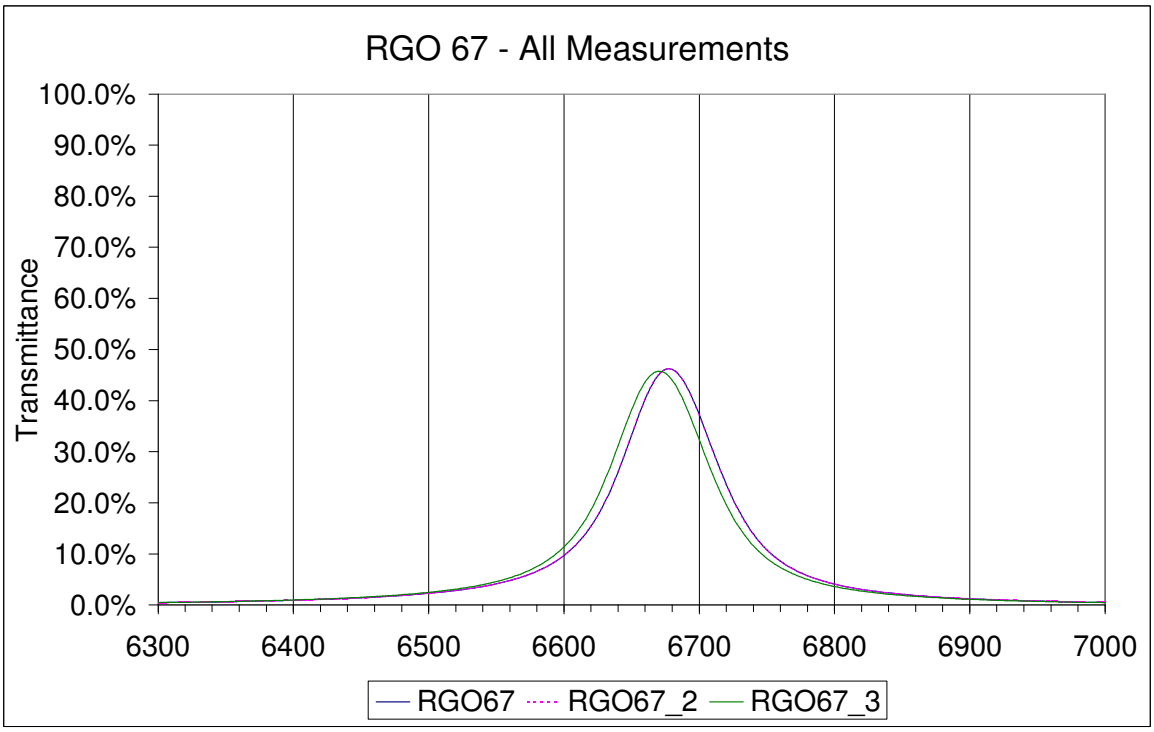

Figure 10 – Transmittance of filter RGO 67

Label	Filter	Point in which measured
H1_1	H_α 1	Near the filter's **center**
H1_2	H_α 1	**Same** point as H1_1
H1_3	H_α 1	**Off center**
H2_1	H_α 2	Near the filter's **center**
H2_2	H_α 2	**Same** point as H2_1
H2_3	H_α 2	**Off center**
H3_1	H_α 3	Near the filter's **center**
H3_2	H_α 3	**Off center**
H3_3	H_α 3	Between H3_1 and H3_2
H3_4	H_α 3	**~1/2 radius** from center (almost completely outside the central spot)
H4_1	H_α 4	Near the filter's center
H4_2	H_α 4	Displaced from H4_1 in a direction, **parallel** to the visible rectangle aperture
H4_3	H_α 4	Displaced from H4_1 by **~2/3** of the filter's radius in a direction, **perpendicular** to the visible rectangle aperture
H5_1	H_α 5	Near the filter's **center**
H5_2	H_α 5	Displaced from H5_1 by **~1/3** of the filter's radius in a direction, **parallel** to the visible rectangle aperture
H5_3	H_α 5	Displaced from H5_1 by **~1/2** of the filter's radius in a direction, **perpendicular** to the visible rectangle aperture
H6_1	H_α 6	Near the filter's **center**
H6_2	H_α 6	Displaced from H6_1 by **~1/3** of the filter's radius in a direction, **parallel** to the visible rectangle aperture
H6_3	H_α 6	Displaced from H6_1 by **~1/2** of the filter's radius in a direction, **perpendicular** to the visible rectangle aperture
H7_1	H_α 7	Measured at a point near the filter's **center**
H7_2	H_α 7	Displaced from H7_1 by **~1/3** of the filter's radius in a direction, **parallel** to the visible rectangle aperture
H7_3	H_α 7	Displaced from H7_1 by **~1/2** of the filter's radius in a direction, **perpendicular** to the visible rectangle aperture
H7_4	H_α 7	Near the filter's **center**, but with the red side to the right (in all other cases, unless noted otherwise, the red side was to the left)
H8_1	H_α 8	Near the filter's **center**
H8_2	H_α 8	Displaced from H8_1 by **~1/3** of the filter's radius in a direction, **parallel** to the visible rectangle aperture
H8_3	H_α 8	Displaced from H8_1 by **~1/2** of the filter's radius in a direction, **perpendicular** to the visible rectangle aperture, and with the red side pointing to the right (in all other cases, unless noted otherwise, the red side was to the left).
H9_1	H_α 9	Near the filter's **center** (less than ~1/5 of the radius away from the center)
H9_2	H_α 9	Displaced from H9_1 by **~1/3** of the filter's radius in a direction, **parallel** to the visible rectangle aperture
H9_3	H_α 9	Displaced from H9_1 by **~1/2** of the filter's radius in a direction, **perpendicular** to the visible rectangle aperture
RGO67	RGO 67	Near the filter's **center**
RGO67_2	RGO 67	**Same** point as RGO67
RGO67_3	RGO 67	**Off Center**

Table 3 – Description of Measurements

Figure 11 shows the average transmittance curves of all the filters together:

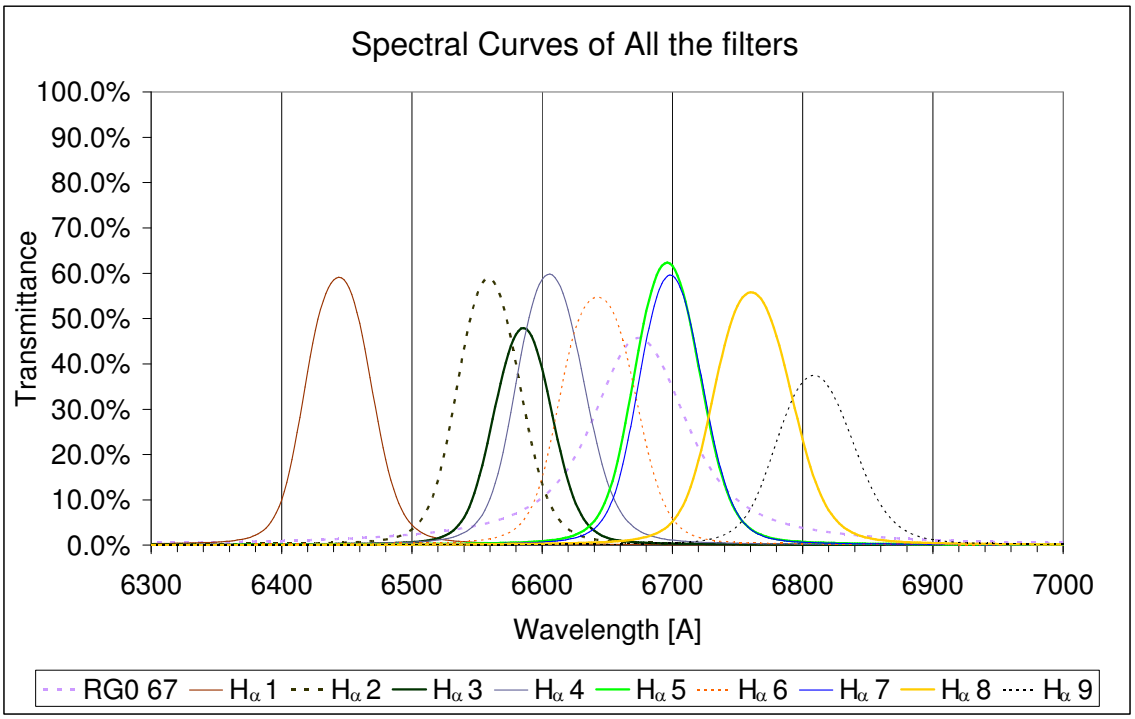

Figure 11 – Filter Comparison

3.3 Calculated values

The Following table lists for each filter its: CWL (central wavelength), FWHM (full width at half maximum), T_{max} (peak transmittance), and an upper limit estimate of the out-of-band transmittance (as explained in section 2):

Filter	CWL [Å]	FWHM [Å]	T_{max}	Out of Band Transmittance (Upper Limit Estimate)
H_α 1	6444 ± 2	58 ± 2	59.1 ± 0.3%	0.05%
H_α 2	6559 ± 2	56 ± 2	58.9 ± 0.3%	0.06%
H_α 3	6585 ± 2	52 ± 2	Variable* (58-31%)	0.03%
H_α 4	6607 ± 2	60 ± 2	Variable* (63-55%)	0.07%
H_α 5	6696 ± 2	58 ± 2	62.4 ± 0.3%	0.07%
H_α 6	Variable* (6640-6646)	66 ± 2	54.8 ± 0.3%	0.06%
H_α 7	Variable* (6697-6702)	56 ± 2	Variable* (60-59%)	0.07%
H_α 8	Variable* (6756-6766)	Variable* (66-70)	Variable* (60-53%)	0.05%
H_α 9	Variable* (6805-6813)	Variable* (64-72)	Variable* (48-32%)	0.03%
RGO 67	Variable* (6678-6671)	86 ± 2	45.7 ± 0.3%	0.05%

Table 4 – Measured Filter Parameters

* - "Variable" refers to situations, were the value varies with the location on the filter's surface. The numbers in parentheses are the range of values that were actually measured (only parts of a filter's surface were tested). The first number refers to the value, measured approximately at the center of the filter. The second number corresponds to the measured point, which is farthest from the center (In all cases, these values seem to approximately behave as monotonous functions of the distance from the center).
A value was declared "variable" in all cases, where its standard deviation for the different measured points exceeded its estimated measurement error.

The measurement errors in CWL and FWHM are ±2Å (the resolution of the spectrometer). The measurement error in the peak transmittance was estimated to be 0.3% (based on repeated measurements of the same points in several filters).

4 Discussion

4.1 Comparison to Older Data

Since the goal of this test was to verify that the filters are not damaged, it makes sense to start by comparing their measured parameters to older data [Almoznino, Kaspi]. This was done in Table 5, which compares the measured CWL (central wavelength) to older values, and Table 6, which makes a

similar comparison of the FWHM (filter width). Older data for T_{max} was found for only five of the filters. Comparison of T_{max} for these filters is presented in Table 7.

Filter	CWL [Å]			
	Current Measurement	Old Measurement	According to Manufacturer	$\Delta_{(Current - Old)}$
H_α 1	6444	6447	6450	-3
H_α 2	6559	6562	6563	-3
H_α 3	6585	6586	6590	-1
H_α 4	6607	6610	6615	-3
H_α 5	6696	6700	6700	-4
H_α 6	6640*	6635	6635	+5
H_α 7	6697*	6697	6680	0
H_α 8	6756*	6760	6760	-4
H_α 9	6805*	6800	6800	+5
RGO 67	6678*	6659	-	+19

Table 5 – CWL Change

* - For filters with CWL that varies in different points along the filter, the value at the center was taken. This is the representative value for comparison, since older measurements were made approximately on the filters' centers.

Filter	FWHM [Å]			
	Current Measurement	Old Measurement	According to Manufacturer	$\Delta_{(Current - Old)}$
H_α 1	58	54	-	+4
H_α 2	56	50	-	+6
H_α 3	52	48	-	+4
H_α 4	60	55	-	+5
H_α 5	58	53	-	+5
H_α 6	66	-	55	+11**
H_α 7	56	-	55	+1**
H_α 8	66*	-	60	+6**
H_α 9	64*	-	65	-1**
RGO 67	86	60	-	+26

Table 6 – FWHM Change

* - For filters with FWHM that varies in different points along the filter, the value at the center was taken. This is the representative value for comparison, since older measurements were made approximately on the filters' centers.

** - In cases, where no data was available for an older measurement, the value $\Delta_{(Current - Manufacturer)}$ replaces $\Delta_{(Current - Old)}$.

Filter	T_{max}		
	Current Measurement	Old Measurement	Ratio (Current/Old)
H_α 1	59.1%	64.4%	0.92
H_α 2	58.9%	67.5%	0.87
H_α 3	57.6%*	66%	0.87
H_α 4	62.6%*	69.7%	0.90
H_α 5	62.4%	70%	0.89

Table 7 – Peak Transmittance Change

* - For filters with T_{max} that varies in different points along the filter, the value at the center was taken. This is the representative value for comparison, since older measurements were made approximately on the filters' centers.

As can be seen from these tables, other than for "RGO 67", the CWL did not change since the older measurements by more than 5Å, or 8% of the FWHM. The CWL of filter "RGO 67" changed more significantly, i.e. by 19Å, or 32% of its older FWHM.

Other than for filters "H_α 6" and "RGO 67", the FWHM did not change by more than 6Å, or 12%. For "H_α 6", and "RGO 67" the change was more significant: 17% and 30% respectively.

T_{max} had decreased significantly (by a factor of 0.87 to 0.92) for the five filters that had older measurement.

Adding this all up, it seems that the filters had somewhat changed since being last measured. This change is reflected in some reduction in the peak transmittance, which probably affects all filters, and in a small change to the CWL and FWHM.

The transmittance reduction should not deem the filters unusable, since its only affect is signal reduction, which can be compensated by increasing the exposure time. However, the large CWL and FWHM change in filter "RGO 67", and to a lesser extent the FWHM change in filter "H_α 6" are suspicious, and should be considered (Strangely, unlike most filters, these two looked perfect in the visual inspection).

4.2 Uniformity

Unfortunately, not all of the filters are uniform along their surface. Apart from visible spots on their silver side, they also exhibit variations in CWL, FWHM and peak transmittance.

CWL variation was detected on five of the filters. The measured variations were up to 10Å, i.e. up to 15% of the FWHM. Variations in FWHM were detected in two of the filters. These were measured to be no more than 8Å, or 13% of FWHM.

Variations in T_{max} were detected in five of the filters. In three of the cases, they were of a factor of down to 0.88, and on the other two, "H_α 3" and "H_α 9", they were of factors of 0.53 and 0.67 respectively.

It's important to note that the above variation values might be somewhat underestimated, since parts of the filters' surfaces were not measured. Particularly, the areas very close to the filter's edges could not be measured for technical reasons. These areas are likely to exhibit slightly increased variations, compared to the variations in the measured off-center points.

Only three of the filters did not exhibit any type of variation in their transmittance curves ("H_α 1", "H_α 2" and "H_α 5"). Filters "H_α 4", "H_α 6", "H_α 7" and "RGO 67" exhibited some variations, and filters "H_α 3", "H_α 8" and "H_α 9" exhibited large variations.

Additionally, some more variations might occur due to the angle of incidence of the beam, as it hits the filter. In this effect, which is characteristic to interference filters, the CWL is shifted to lower wavelengths. This shift gets larger as the beam's angle of incident is increased [Wolfe and Zissis].

Typically the filters will be used in the Wise observatory with f/7 optics [Kaspi], which corresponds to a half cone angle of about 4°. Although the effect of this cone of incidence depends on the specific design of the filters, as well as on the exact intensity distribution, a typical effect is in the order of 10^{-3} of the CWL [Wolfe and Zissis], i.e. roughly 7Å, or 15% of the FWHM. For larger F numbers (for example, f/13.5 of the two-star photometer) this effect will be smaller.

The exact effect of these variations is hard to calculate, and depends greatly on the details of the telescope's optical system. Specifically, it depends on the geometry and intensity distribution of an object's beam as it passes through the filter. If, for example, more of the intensity passes through the edges of the filter, the transmittance curve will be more similar to that of the points measured close to the filter's edges.

Luckily however, the effects of CWL variations due to off-center point and due to the angle of incidence are reversed in direction for most filters (all but "RGO 67"). This might work to our advantage, when the measured object's beams are centered on the filter. In such a case, the beam that passes through the filter's center has a zero angle of incidence, and therefore is not shifted. The beams that pass away from the filter's center will encounter an increased CWL due spatial variations (for "H_α 6", "H_α 7", "H_α 8" and "H_α 9"), but since their angle of incidence is non zero they will be somewhat shifted back to a lower CWL. As the beam passes farther from the filter's center, both reversed effects will be increased.

4.3 Blocking

As for the quality of blocking outside the transmittance band, not a lot can be concluded with great confidence. Uncertainty is mostly due to the fact that blocking was tested only for a small part of the wavelength range, which Silicon CCD's respond too.

On first look blocking seems very good, being lower by at least 3 OD (orders of magnitude) from the peak transmittance. This assures that emission lines of the same order of magnitude as the H_α line would not affect the measurement.

However, compared to continuum radiation, the measurements performed in this test do not seem perfect. Since typically a Silicon CCD responds to wavelengths from ~3,000Å to ~11,000Å (a width of ~8,000Å), a blocking of 3 OD still transmits continuum radiation which is equivalent to an increase of roughly 10Å in the FWHM.

Luckily, the 3 OD blocking is only an upper limit, and the expected blocking is much lower (since the blocking was tested relatively close to the transmitting band, where the transmittance still seems to decrease with distance from the CWL).

4.4 Velocity Range

Each of the filters has its unique transmittance range, which corresponds to a unique range of possible redshifts, in which the H_α line can be measured.

The wavelength of the non shifted H_α line is 6562.8Å [Herter]. Since the redshifts are small (z<0.05), the corresponding receding velocity can be simply calculated according to:

(1) $$v = c \cdot z = c\left(\frac{\lambda}{\lambda_{H_\alpha}} - 1\right)$$

Where:

- v - Receding velocity
- c - Speed of light
- z - Redshift
- λ - The wavelength, in which the H_α line is observed
- λ_{H_α} - The wavelength, in which the H_α line is emitted (6562.8Å)

Since each filter transmits a range of wavelengths, it also corresponds to a range of receding velocities, which "width" is:

(2) $$\Delta v = c \cdot \frac{\Delta\lambda}{\lambda_{H_\alpha}}$$

Where:

- Δv - The width of the range of receding velocities
- $\Delta\lambda$ - The width of the range of transmitted wavelengths

Now, the uncertainty in the effective CWL and FWHM of the filters, discussed in section 4.2, has to be considered. Variations across a filter's surface amount in an increase of CWL of up to 15%×FWHM, and an increase in FWHM of up to 13%. Further CWL shifts due to angle of

incidence were roughly estimated as -15%×FWHM. To compensate for this, safety margins of 20%×FWHM (from each side) were kept from the original FWHM, i.e. calculations were based on: $\Delta\lambda$=0.6×FWHM.

Results according to this definition (rounded to 100km/s) are listed in the following table:

Filter	Velocity Range [km/s]	
	From	To
H_α 1	-6200	-4600
H_α 2	-900	+600
H_α 3	300	1700
H_α 4	1200	2800
H_α 5	5300	6900
H_α 6	2700	4500
H_α 7	5500	7000
H_α 8	8100	10000
H_α 9	10300	12200
RGO 67	3900	6300

Table 8 – Velocity Ranges

As can be seen from this table, the filters cover all the velocity range from -900km/s to +7000km/s with some overlaps. The range 8100km/s to 12200km/s is mostly covered.

However, it should be noted that these velocity ranges were calculated for high levels of signal to background ratio (H_α to continuum), i.e. for wavelengths around the peak of the transmittance curves. This means that the velocity ranges can be widened, if one accepts lower signal to background ratios.

5 Conclusion

All of the tested filters were found to be usable.

Some variations were found between current and older measured transmittance curves, but these do not indicate severe faults.

However, some of the filters show significant variations in CWL and FWHM across their surface. This, along with wavelength shifts due to the light's distribution in the angle of incidence space, should be considered.

Therefore, in order to minimize measurement errors (as discussed in section 4.2), it is advised to make all measurements with the object centered in the field of view. In this way, the effective transmittance curve will be, if not accurately known, at least similar between measurements.

6 References

Almoznino - E. Almoznino, "Star Formation in Late-Type Dwarf Galaxies in the Virgo Cluster", PhD thesis, Tel-Aviv University, 1994.

Heller - A. B. Heller, "Structure and Star Formation Regimes of Low Surface Brightness Dwarf Irregular Galaxies in the Virgo Cluster", PhD thesis, Tel-Aviv University, 2001.

Herter – T. Herter, "The Nature of the Universe", "Astronomy 101/103" Course delivered at Cornell University, USA, "Lecture 8: The Hydrogen Atom", http://instruct1.cit.cornell.edu/courses/astro101/lec08.htm, 2006.

Kaspi - S. Kaspi, P. A. Ibbetson, E. Mashal and N. Brosch, "Wise Observatory Manual", School of Physics and Astronomy and the Wise Observatory, Tel-Aviv University, 1999.

Wolfe and Zissis – W. L. Wolfe and G. J. Zissis, "The Infrared Handbook", prepared by IRIA, center of the Environmental Research Institute of Michigan, USA, 1978.